

## MICROSTRUCTURAL, ELECTRICAL AND OPTICAL PROPERTIES OF DC REACTIVE MAGNETRON SPUTTERED ZINC ALUMINUM OXIDE THIN FILMS FOR OPTOELECTRONIC DEVICES

B.RAJESH KUMAR<sup>a,b\*</sup>, T. SUBBA RAO<sup>b</sup>

<sup>a</sup>*Department of Physics, Sri Venkateswara University, Tirupati-517502, A.P, India*

<sup>b</sup>*Department of Physics, S.K.University, Anantapur-515003, A.P, India*

Zinc Aluminum Oxide (ZAO) thin films have been deposited on glass substrates by DC reactive magnetron sputtering technique. The structural, electrical and optical properties of ZAO thin films deposited with various substrate temperatures were investigated. XRD patterns exhibits ZAO thin films had a diffraction peak corresponding to (0 0 2) preferred orientation with the c-axis perpendicular to the substrate surface. The preferred orientation is due to the lowest surface free energy for (0 0 2) plane. The minimum resistivity of  $5.14 \times 10^{-4} \Omega \cdot \text{cm}$  is obtained for the thin film deposited at substrate temperature of 300 °C. Optical absorption edge of ZAO thin films has a significant blue shift to the region of higher photon energy. The average transmission of ZAO films in the visible range is > 80%. The optical direct band gap values of ZAO films increased with increasing substrate temperature and this may be attributed to Burstein-Moss shift.

(Received April 20, 2012; Accepted May 11, 2012)

*Keywords:* Transparent conducting oxide; DC reactive magnetron sputtering; Substrate temperature; Electrical properties; Optical properties

### 1. Introduction

Doped ZnO is among few metal oxides which can be potentially used as transparent conducting oxides (TCOs) [1]. The advantages of ZnO are the wide band gap of 3.3 eV, low resistivity, high transparency in the visible range, high light trapping characteristics and low preparation costs. The n-type dopants used in ZnO are mainly  $\text{In}^{3+}$ ,  $\text{Al}^{3+}$ ,  $\text{B}^{3+}$ ,  $\text{Ga}^{3+}$  [2-5]. Among all these dopants Al is relatively a cheaper, abundant and non-toxic material and hence Al-doped ZnO films can be prominent, low – cost substitute for high cost Tin doped  $\text{In}_2\text{O}_3$  (ITO) films in all TCO applications. Transparent and conductivity Zinc Aluminum Oxide (ZAO) films are now being considered for manufacturing transparent electrodes in flat panel displays, solar cells and organic light emitting diodes due to the large availability and low cost of the materials for large area applications in optoelectronic devices. The magnetron sputtering process has the advantage of facilitating the growth of TCO films due to the high growth rate and large area uniformity [6, 7].

Reactive sputtering using metallic targets is the most promising technique because of its high deposition rate, large area scalability, and easy preparation of a large size as well as a high conductivity and visible transmittance [8]. The growth temperature plays a major role for the determination of thin film properties. The present work is focused on influence of substrate temperature on structural, electrical and optical properties of ZAO thin films. This paper reports the first observation of ZAO thin films sputtered by taking two individual metal targets of Zn and Al.

### 2. Experimental details

Zinc Aluminum Oxide (ZAO) thin films were prepared by DC reactive magnetron sputtering at various substrate temperatures. High purity of Zn (99.999%) and Al (99.99%) targets

---

\* Corresponding author: rajphyind@gmail.com

with 2 inch diameter and 4 mm thickness are used for deposition on glass substrates. The base pressure in chamber was  $6 \times 10^{-6}$  Torr and the distance between target and substrate was set at 60 mm. The glass substrates were ultrasonically cleaned in acetone and ethanol, rinsed in an ultrasonic bath in deionized water for 15 min, with subsequent drying in an oven before deposition. High purity (99.99%) Ar and O<sub>2</sub> gas was introduced into the chamber and was metered by mass flow controllers (Model GFC 17, Aalborg, Germany), the flow rate fixed for Ar is 25 sccm. The O<sub>2</sub> flow rate is fixed at 2 sccm and the deposition time is 30 min. Deposition was carried out at a working pressure of  $3 \times 10^{-6}$  Torr after pre-sputtering with argon for 10 min. The depositions were carried out at substrate temperatures varied from room temperature (RT) to 350 °C. The deposition conditions were optimized in such a way that the ZAO films exhibited a good surface roughness for light scattering and low resistivities. Film thickness was measured by Talysurf thickness profilometer. The resulting thicknesses of the films are found to be ~ 400 nm. X-ray diffraction (XRD) patterns of the films were recorded with the help of Philips (PW 1830) X-ray diffractometer using CuK $\alpha$  radiation. The tube was operated at 30 KV, 20mA with the scanning speed of 0.030(2 $\theta$ )/sec. Surface morphology of the samples has been studied using HITACHI S-3400 Scanning Electron Microscope (SEM). The elementary composition of the films was determined from Energy Dispersive X-ray Spectroscopy (EDS, Horiba EMAX, 137 eV). Optical transmittance of the films was recorded as a function of wavelength in the range of 300 – 1200 nm using JASCO Model V-670 UV-Vis-NIR spectrophotometer (Japan).

### 3. Results and discussion

Fig.1 shows the XRD patterns of ZAO films deposited on glass substrates from room temperature (RT) to 350 °C. X-ray diffraction analysis shows that the deposited films have a preferential growth along the c-axis of the hexagonal structure. The preferred orientation is due to the lowest surface free energy for (0 0 2) plane [9-11]. The diffraction peak position 2 $\theta$  shifts from 34.30° to 34.40° at room temperature (30 °C) - 200 °C and then decreases to 34.37° at higher substrate temperatures. These shifts indicate the presence of a stress state in deposited films. This can be due to the incorporation of Al as dopant in the ZnO lattice due to the different ionic radii of Al<sup>3+</sup> and Zn<sup>2+</sup>. The stress is reduced at higher substrate temperatures which can be explained in terms of thermal relaxation. From XRD patterns the full width at half maximum (FWHM) decreases from 0.23° to 0.16° at 200 °C but slightly increases to 0.20° at 350 °C. The crystallite size of the deposited films has been calculated from FWHM of (0 0 2) peak by using Scherrer formula [12]. The crystallite size increases from 38 to 52 nm with increase of substrate temperature upto 200 °C. Then it decreases to 41.6 nm at substrate temperature of 350 °C. The increase of crystallite size with substrate temperature is attributed to the improvement of ZAO crystallinity by the coalescence of small crystallites [13].

The film stress parallel to the film surface is calculated from the biaxial strain model [14]. The negative value in the stress corresponds to compressive stress. The intrinsic stress originates from the growth process as a result of ingrown defects or structural mismatch between film and substrate. As shown in Fig. 2 the compressive stress increases with increase of substrate temperature. The maximum stress is obtained for the film deposited at 300 °C due to the existence of re-crystallization. After 300 °C the internal stress in the films was decreased due to increase of mobility, it may be due to effect of high substrate temperature. The atoms can easily diffuse from one position to another and shift to a more equilibrium position, thus decrease the compressive stress. These results are in agreement with earlier report [15].

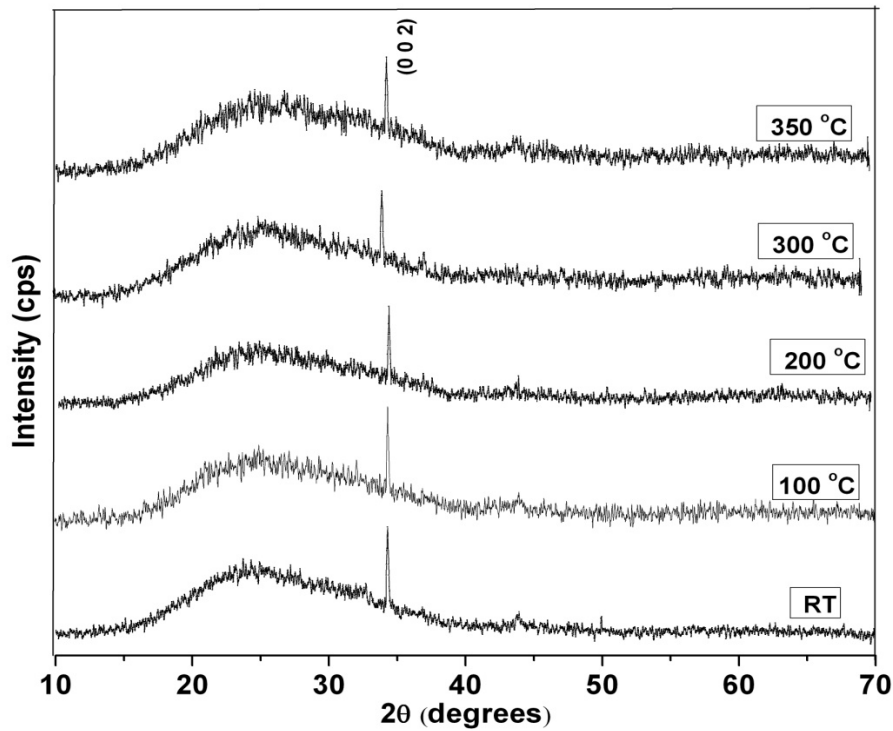


Fig. 1 XRD patterns of ZAO thin films deposited at different substrate temperatures.

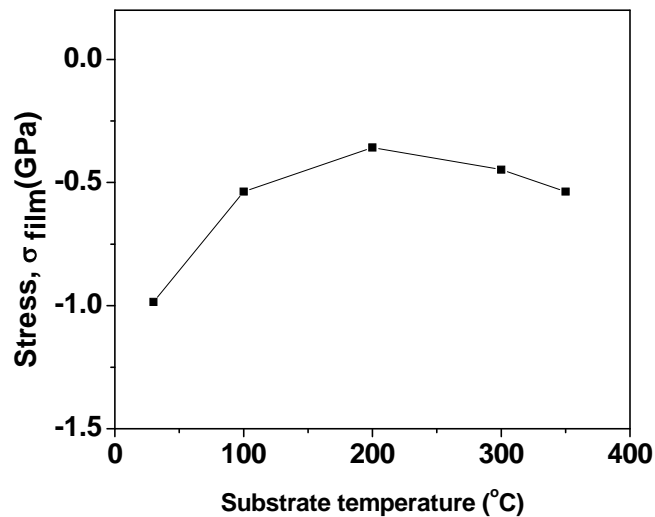


Fig. 2 Variation of residual stress with substrate temperature.

SEM images of ZAO thin films deposited at different substrate temperatures are shown in Fig. 3. The grain sizes increase with increase of substrate temperature and in the range of 0.4 – 1  $\mu\text{m}$ . Higher substrate temperature provides energy for surface atoms to enhance mobility that can improve the quality of films crystallinity. Higher substrate temperatures enhanced mobility but also caused the re-evaporation of poorly combined structures that made the structures irregular. This contributed to the film's irregular surface morphology. Increasing substrate temperature produced larger grains. Fig. 4 shows the EDS plot with compositional elemental data for ZAO films deposited at various substrate temperatures.

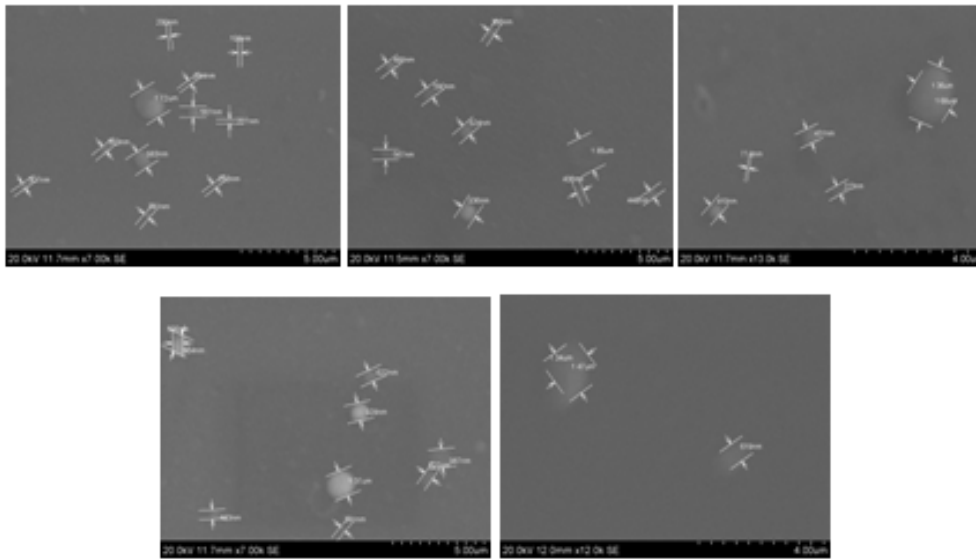


Fig. 3 SEM images of ZAO thin films deposited at the substrate temperatures of (a) Room temperature (RT) (b) 100 °C (c) 200 °C (d) 300 °C and (e) 350 °C.

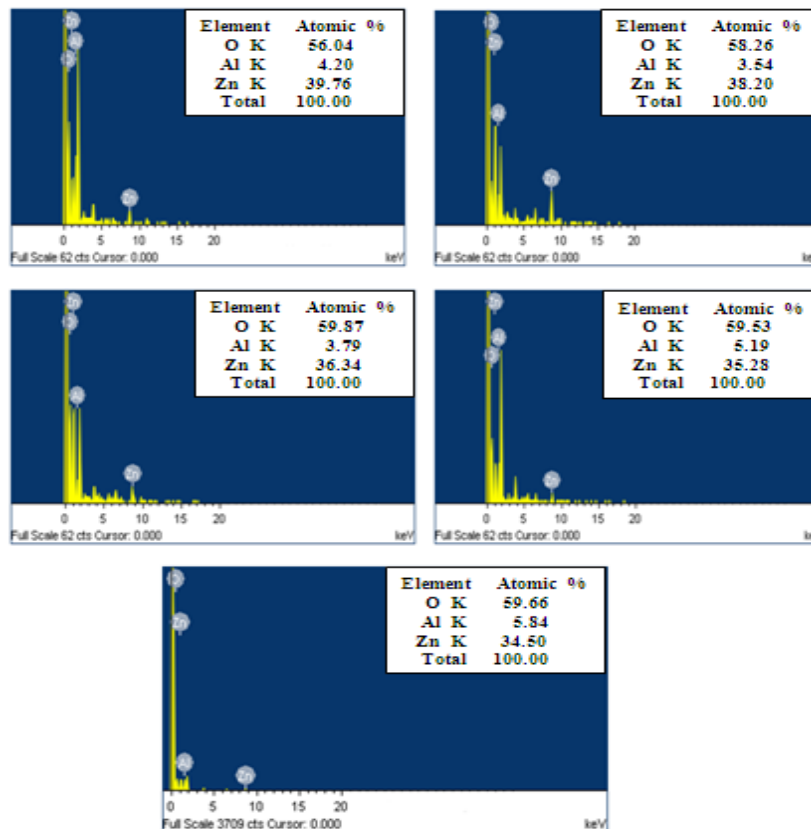


Fig. 4 EDS plot for ZAO thin films deposited at various substrate temperatures.

The electrical resistivity of ZAO films was investigated by four-point probe method at room temperature. The resistivity of ZAO thin films deposited at various substrate temperatures is shown in Fig 5. The resistivity decreases with increase of substrate temperature. The resistivities values are varied from  $2.3 \times 10^{-3} \Omega \cdot \text{cm}$  to  $8.72 \times 10^{-4} \Omega \cdot \text{cm}$ . The lowest resistivity of  $5.14 \times 10^{-4} \Omega \cdot \text{cm}$  is obtained for the thin films deposited at 300 °C and then it slightly increases to  $8.72 \times 10^{-4} \Omega \cdot \text{cm}$  for 350 °C. In ZAO thin films the conductivity is better to pure ZnO films owing to  $\text{Al}^{3+}$  ions

at substitutional sites  $Zn^{2+}$  site. The decrease of resistivity with increase of substrate temperature is due to the enhancement of film crystallinity, carrier concentration and carrier mobility. The higher the crystal orientation the lower will be resistivity. This is due to the reduction in the scattering of the carriers at the grain boundaries and crystal defects.

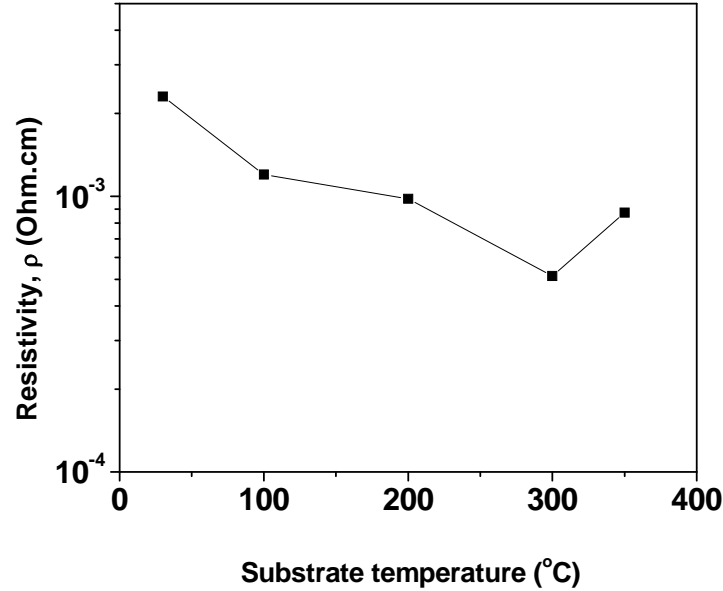


Fig. 5 Variation of electrical resistivity as a function of substrate temperature.

The sheet resistance of the film ( $R_s$ ) was calculated using the equation

$$R_s = \frac{\rho}{t} \quad \Omega/\text{sq} \quad (1)$$

where  $t$  is the film thickness.

The sheet resistance ( $R_s$ ) for ZAO thin films deposited at substrate temperatures of RT, 100 °C, 200 °C, 300 °C and 350 °C are obtained to be 57.5, 30, 24.5, 13 and 22  $\Omega/\text{sq}$  respectively.

Fig. 6 shows the optical transmittance spectra of ZAO thin films. The average transmittance of all the films in the visible range is >80%. The maximum optical transmittance is obtained for the thin film deposited at 350 °C. The increase of optical transmittance of ZAO film with increasing substrate temperature can be ascribed to the weakening of scattering and absorption of light because of the increase of grain size. The decrease of transmittance at room temperature may be attributed to the increased scattering of photons by crystal defects created by doping. The free carrier absorption of the photons may also contribute to the observed reduction in the optical transmission of heavily doped films [16]. The absorption edge of the transmittance for the films deposited at various substrate temperatures shifts to shorter wavelength from 352 nm to 371 nm (blue shift). The blue shift of the absorption edge with deposition temperature is mainly attributed to the Burstein-Moss effect, since the absorption edge of a degenerate semiconductor is shifted to shorter wavelength with increasing carrier concentration.

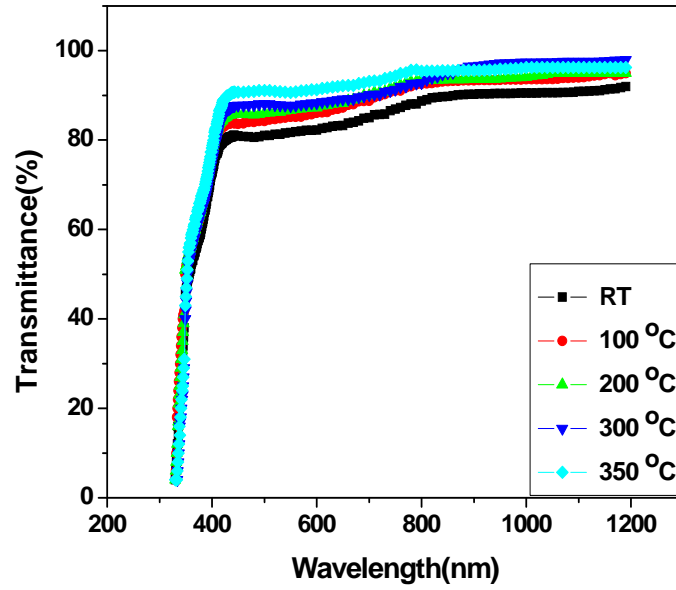


Fig. 6 Optical transmittance spectra of ZAO films as a function of wavelength at different substrate temperatures

The optical band gap,  $E_g$  is determined from the dependence of absorption coefficient values ( $\alpha$ ) on the photon energy, using Tauc's relation [17]

$$(\alpha h\nu) = B(h\nu - E_g)^n \quad (2)$$

where B is a parameter that depends on the transition probability  $E_g$  is the optical band gap energy of the material,  $h\nu$  is the photon energy and n is an index that characterizes the optical absorption process and is theoretically equal to 2 and  $\frac{1}{2}$  for indirect and direct allowed transitions respectively.

The optical band gap of ZAO films was evaluated from the plots of  $(\alpha h\nu)^2$  versus  $h\nu$  shown in Fig. 7. The  $E_g$  increases with increase of substrate temperature from 3.34 to 3.52 eV. The observed widening of band gap is due to Burstein-Moss effect. The Burstein-Moss effect explained the broadening of band gap energy with the increasing of carrier concentration. It is due to the donor electron occupying the states at the bottom of the conduction band since the Pauli principle prevent donor electron from being double occupied. In that case, measured optical band gap energy is equal to the sum of intrinsic band gap energy plus energy of state occupied by the donor electron at the conduction band which caused band gap widening. Similar behavior is reported in the previous literature work [18].

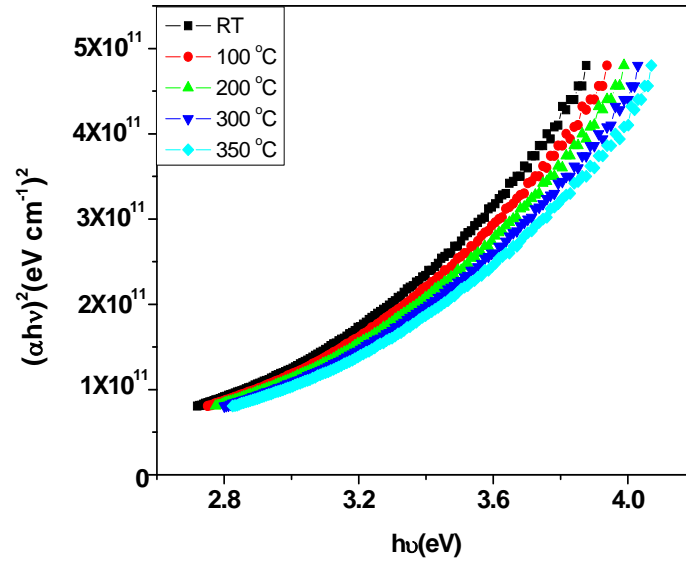


Fig. 7 Plots of  $(\alpha hv)^2$  versus photon energy  $hv$  of ZAO thin films with various substrate temperatures

The energy band gap widening  $\Delta E_g$  is related to carrier concentration through the following equation [19]

$$\Delta E_g = \left( \frac{h^2}{8m^*} \right) \left( \frac{3N}{\pi} \right)^{\frac{1}{3}} \quad (3)$$

Where  $h$  is the Planks constant,  $m^*$  is the electron effective mass in conduction band, and  $n$  is the carrier concentration. From equation (4) it can be found that the energy band gap widening increases with increase of carrier concentration of ZAO thin films. The carrier concentration of ZAO thin films are determined from equation (3) and it is found to be in the range of  $6.75 \times 10^{19} \text{ cm}^{-3}$  –  $8.70 \times 10^{20} \text{ cm}^{-3}$ .

Figure of merit ( $\Phi$ ) is the quantity to judge the quality of the transparent conducting oxide films. The figure of merit of the films was evaluated from the optical transmittance and sheet resistance ( $R_s$ ) using the Haacke's relation [20].

$$\Phi (\Omega^{-1}) = \frac{T^{10}}{R_s} \quad (4)$$

where  $T^{10}$  is the average optical transmittance and  $R_s$  is the sheet resistance. The best figure of merit with  $1.72 \times 10^{-2} \Omega^{-1}$  and sheet resistance of  $13 \Omega/\text{sq}$  is obtained for the film deposited at  $300^\circ\text{C}$ .

#### 4. Conclusions

ZAO thin films have been deposited on glass substrates by DC reactive magnetron sputtering technique. The substrate temperature is varied from room temperature to  $350^\circ\text{C}$ . The films are oriented along the  $c$ -axis of the hexagonal structure. The film resistivity decreases with increase of substrate temperature upto  $300^\circ\text{C}$  and then slightly increases at  $350^\circ\text{C}$ . The minimum resistivity of  $5.14 \times 10^{-4} \Omega.\text{cm}$  and an average transmittance of 86% are obtained for the thin film deposited at  $300^\circ\text{C}$ . From these results we conclude that ZAO films are promising for optoelectronic applications such as transparent electrodes for solar cells, flat panel displays and organic light-emitting diodes.

### Acknowledgements

The authors are thankful to UGC, New Delhi, India for financial support under the major research project (F.NO.37-346/2009, SR).

### References

- [1] B.-Y.Oh, M.-C.Jeong, D.-S.Kim, W.Lee, J.-M.Myoung, *J.Cryst. Growth* **281**, 475 (2005).
- [2] J.Jie, G.Wang, X.Han, Q.Yu, Y.Lia, G.Li, J.G.Hou, *Chem.Phys.Lett.* **387**, 466 (2004).
- [3] C David, T Girardeau, F Paumier, D Eyidi, B Lacroix, N Papathanasiou, B P Tinkham, P Guérin and M Marteau, *J.Phys.:Condens.Matter* **23**, 334209 (2011).
- [4] S.Y.Bae, C.W.Na, J.H.Kang, J.Park, *J.Phys.Chem. B* **109**, 2526 (2005).
- [5] A K K Kyaw, X W Sun, J L Zhao, J X Wang, D W Zhao, X F Wei, X W Liu, H V Demir, T Wu *Appl.Phys.* **44**, 045102 (2011).
- [6] J.Kim, J.H.Yun, S.W.Jee, Y.C.Park, M.Ju, S.Han et al., *Mater Lett.* **65**, 786 (2011).
- [7] B.H.Kong, M.K.Choi, H.K.Cho, J.H.Kim, S.Baek, J.H. Lee, *Electrochem Solid-State Lett.* **13**, K12 (2010).
- [8] S.J.Jung, B.M.Koo, Y.H.Han, J.J.Lee, J.H.Joo, *Surf. Coat.Techn.* **200**, 862 (2005)
- [9] N.Fujimura, T.Nishihara, S.Goto, J.F.Xu, T.Ito, *J.Cryst. Growth* **130**, 269 (1993).
- [10] K.H.Kim, R.A.Wibowo, B.Munir, *Mater. Lett.* **60**, 1931 (2006).
- [11] J.F.Chang, L.Wang, M.H.Hon, *J.Cryst. Growth* **211**, 93 (2006).
- [12] L.Sagalowicz, G.R.Fox, *J.Mater.Res.* **14**, 1876 (1999).
- [13] S.M.Park, T.Ikegami, K.Ebihara, *Thin Solid Films* **513**, 90 (2006).
- [14] A.Segmuller, M.Murakami, R.Roscoberg, *Analytical Techniques for Thin Films*, Academic Press, Boston, 143 (1988).
- [15] W.Tang, D.C.Cameron, *Thin Solid Films* **238**, 83 (1994).
- [16] J.P.Upadhyay, S.R.Viswakarma, H.C.Prasad, *Thin Solid Films* **109**, 195 (1989).
- [17] J. Tauc, R. Grigorovici, A. Vancu, *Physica Status Solid* **15**, 627 (1966).
- [18] Xue-Yong Li, Hong-Jian Li, Zhi-Jun Wang, Hui Xia, Zhi-Yong Xiong, Jun-Xi Wang, Bing-Chu Yang, *Optical Communications* **282**, (2009) 247.
- [19] F.Urbach, *Phys.Rev.* **92**, 1324 (1953).
- [20] G. Haacke, *J. Appl. Phys.* **47**, 4086 (1976).